Applied Physics A (2020) 126:418
https://doi.org/10.1007/s00339-020-03559-6

Applied Physics A
Materials Science & Processing

S.I. : CURRENT STATE-OF-THE-ART IN LASER ABLATION

Pure copper layer formation on pure copper substrate using multi-beam laser cladding system with blue diode lasers

Takahiro Hara[1] · Yuji Sato[2] · Ritsuko Higashino[2] · Yoshinori Funada[3] · Tomomasa Ohkubo[4] · Kento Morimoto[1] · Nobuyuki Abe[2] · Masahiro Tsukamoto[2]

Received: 15 October 2019 / Accepted: 16 April 2020 / Published online: 14 May 2020

Abstract
In electrical and mechanical industries, forming a pure copper layer on various substrates would improve the performance of automotive motors, batteries, etc. However, the formation of a pure copper layer has yet to be reported on a pure copper substrate. Here, a pure copper layer is formed on a pure copper substrate (C10200) using a multi-beam laser cladding system with blue diode lasers. The powder mass efficiency increases with the laser intensity. These results are used to construct a powder temperature model. At a laser intensity of 6.5×10^4 W/cm^2, 9.65% of the powder forms a copper layer. In the supplied powder, approximately 5% of the powder is melted on the fly. In addition, about 5% of the powder is melted after trapping on the substrate. Hence, melting powder on the fly and melting the trapped powder on the substrate form the copper layer.

Keywords Blue diode laser · Laser cladding · Multi-beam laser cladding · Pure copper · Powder temperature

1 Introduction

Pure copper has high thermal and electrical conductivities [1]. Forming a pure copper layer improves the performances of the electrical and mechanical components [2–4]. Common methods to form a material layer on the target substrate include thermal spraying, arc welding, and plasma transferred arc welding. However, they have some problems. Thermal spraying is suitable for rapid processing, but the adhesive strength is weak because it is mechanically joined by the anchor effect. Although arc welding and plasma transferred arc welding have good adhesive strength between the substrate and the layer, the excessive heat input results in a large dilution [5–7]. Therefore, we focus on the laser cladding method using a powder. It produces cladding layers on the substrate by melting a powder material via laser irradiation to form a dense and highly pure layer. Hammati et al. [8] reported dilution in the laser cladding process and showed that the hardness of the layer decreases as the dilution ratio increases. Because dilution is a serious problem even in laser cladding, many studies have investigated it. In the conventional method, the laser is irradiated perpendicular to the substrate surface. Then powders are supplied to the focal point from a powder nozzle in a processing head. To melt the unheated powder, a large molten pool must be formed because some powder is unheated on the fly [9–12]. In contrast, it is possible to uniformly heat the powder using multiple lasers. The powder can be melted without a large molten pool, and the powder trapped on the thin molten layer can form the material layer by laser irradiation [13–15]. Hence, it is important to form a stable molten layer on the substrate.

However, it is difficult to form a stable molten layer on pure copper substrates using a laser at the near-infrared (NIR) wavelength range of 900–1100 nm, which is used for conventional laser cladding. The light absorptivity of copper at the NIR wavelength is only 10% under room temperature [16]. Ernie et al. [17] showed that the light absorptivity of pure copper depends on the temperature of the material. When the laser is irradiated on a pure copper substrate at a

✉ Takahiro Hara
hara@jwri.osaka-u.ac.jp

[1] Graduate School of Engineering, Osaka University, 1-1 Yamadaoka, Suita, Osaka 565-0871, Japan

[2] Joining and Welding Research Institute, Osaka University, 11-1 Mihogaoka, Ibaraki, Osaka 567-0047, Japan

[3] Industrial Research Institute of Ishikawa, 2-1 Kuratsuki, Kanazawa, Ishikawa 920-8203, Japan

[4] Department of Mechanical Engineering, Tokyo University of Technology, 1404-1 Katakuramachi, Hachioji, Tokyo 192-0982, Japan

wavelength of 1000 nm, the reflectivity at room temperature (21 °C) is 96%, but it greatly decreases to 76.3% at 200 °C. Hence, the absorbed energy to the substrate increases as the substrate temperature increases.

Morimoto et al. [18] reported welding a pure copper sheet using a fiber laser at a wavelength of 1090 nm. As a result, the behavior of the molten pool is unstable during laser irradiation. In general, the light reflectivity of metal decreases as the wavelength becomes shorter [16]. The light reflectivity at a 450 nm wavelength of pure copper is only 34%, but is 96% for near infrared lasers. The reflectivity is constant from 21 to 200 °C, indicating that a blue diode laser is superior to form a stable molten layer. Sato et al. installed six modules of 20-W blue diode laser in a multi-beam laser cladding system and achieved a total output of 100 W at the processing point. A pure copper layer forms on a stainless-steel substrate with this system [19–22]. The penetration depth depends on the laser intensity. However, heating of the powder by laser irradiation is not fully discussed. Because pure copper has a high thermal conductivity, it is difficult to melt a pure copper substrate with a 100-W-class blue diode laser cladding system. Consequently, there are no reports about pure copper formation on a pure copper substrate with blue diode lasers.

In this study, two modules of a 100-W class blue diode (total output power of 200 W) are installed into a multi-beam laser cladding system. A pure copper layer is formed on a pure copper substrate. The model of flying powder in laser dual-beam laser cladding is constructed, and the melting efficiency of the powder is calculated with this model. Comparing the experimental results with the results calculated from the model, the mechanism of layer formation is clarified.

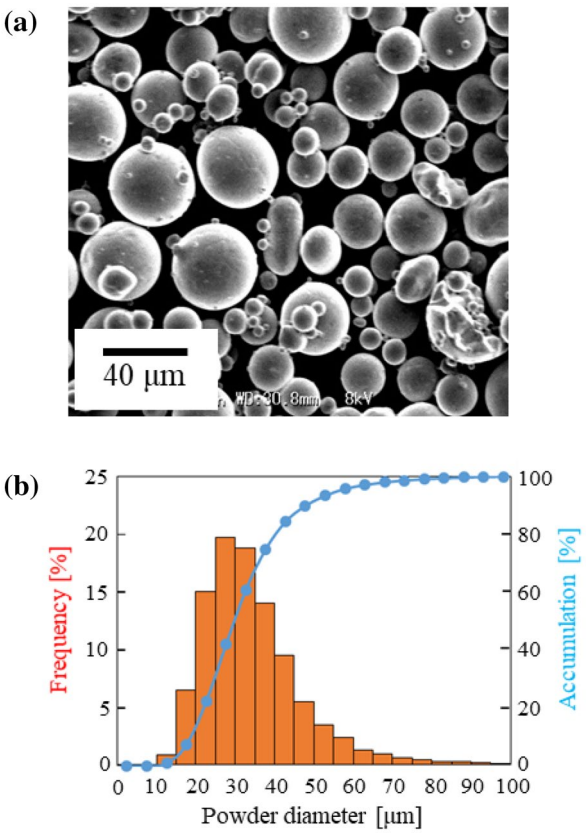

Fig. 1 SEM image of **a** pure copper powder and **b** distribution of the powder diameter

2 Experimental procedures

2.1 Material property

Pure copper powder (Sanyo Special Steel) with a 99.99% purity was prepared by a gas atomized method. The powder had a spherical shape and particle size distribution of 10–60 μm. The average particle size was 34 μm, and the standard deviation was 12 μm (Fig. 1). The substrates were oxygen-free copper (C10200) plates with dimensions of 10 mm × 7 mm × 0.5 mm.

2.2 Copper layer formation using a multi-beam laser cladding system

Figure 2 shows (a) a schematic diagram of the multi-beam laser cladding system and (b) laser beam profile at the focal point. This system was equipped with two modules of a 100-W class blue diode laser (Blue Impact, Shimazu). Each laser beam was guided to the processing head by a optical fiber and combined at a focal point with a focusing lens. The laser spot diameter was set at 534 μm in the X direction and 480 μm in the Y direction at the full width at half maximum. For the focal point, pure copper powder was supplied at 13 mg/s from the supply nozzle in the center of the processing head. The pure copper powder was continuously melted and formed a 5-mm-long pure copper layer. Table 1 shows the experimental conditions. The copper layer was conducted between the laser intensity of $4.2 \times 10^4 \sim 6.5 \times 10^4$ W/cm^2.

The copper-coated sample was cut using a microcutter, filled with a resin, polished, and chemically etched. The surface and cross section were observed using a digital microscope (VHX-3000, Keyence) to measure the cross-sectional area. In addition, the powder mass efficiency e_p is calculated as

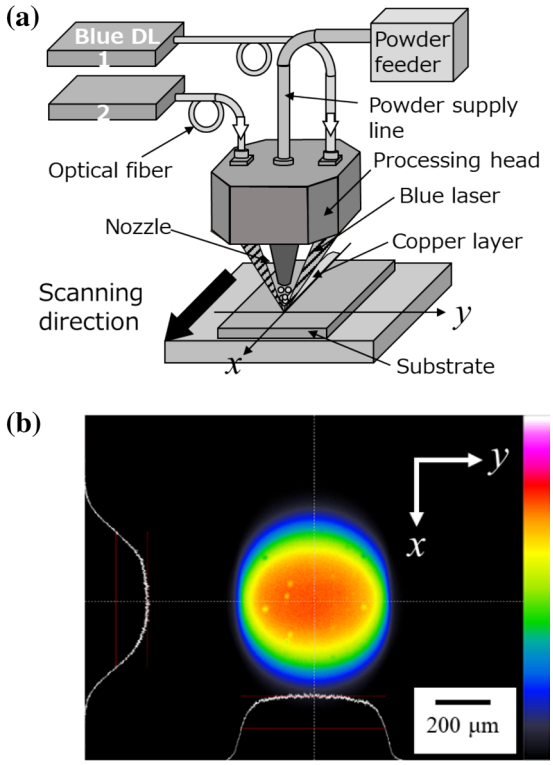

Fig. 2 Schematic of **a** copper layer formation and **b** laser beams profile at the processing point

Table 1 Experimental conditions

Laser wavelength [nm]	450
Laser intensity [W/cm^2]	$4.2 \sim 6.5 \times 10^4$
Scanning speed [mm/s]	1.5
Powder feed rate [mg/s]	13

$$e_p = \frac{\rho \cdot S_{layer} \cdot v_{laser}}{m_p}$$

where ρ is the density of pure copper, S_{layer} is the cross-sectional area of the pure copper layer, v_{laser} is the laser scanning speed, and m_p is the powder feed rate.

3 Results

Figure 3 shows the cross sections of the pure copper layer on the pure copper substrate. At a laser intensity of 4.2×10^4 W/cm^2 or less, the pure copper layer was detached from the substrate, although the pure copper powder was melted and deposited on the substrate. At a laser intensity of 5.1×10^4 W/cm^2, the layer was locally bonded to the substrate. At a laser intensity of 5.9×10^4 W/cm^2, the layer was completely bonded to the substrate with a width of 450 μm, which was smaller than the laser spot diameter. At a laser intensity of 6.5×10^4 W/cm^2, the layer had a 620 μm width, which was larger than the laser spot diameter. Figure 4 shows the surface image and cross-sectional image of laser irradiated

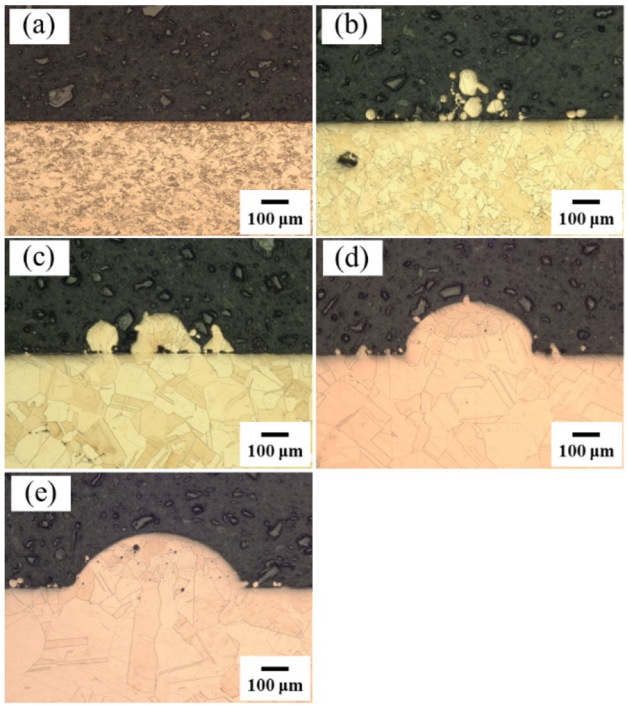

Fig. 3 Surface image of C1020P sample **a** before laser irradiation and after laser irradiation at an intensity of **b** 4.2×10^4 W/cm^2, **c** 5.1×10^4 W/cm^2, **d** 5.9×10^4 W/cm^2 and **e** 6.5×10^4 W/cm^2.

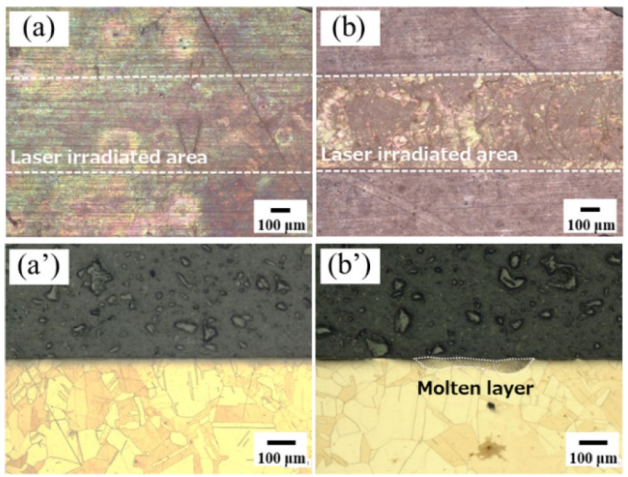

Fig. 4 Surface and cross-sectional image of C1020P sample after laser irradiation without pure copper powder

substrates without a powder supply (bead-on test). At a laser intensity of 4.2×10^4 W/cm^2 or less, the substrate surface did not have a melting mark and the region where the crystal grains changed on the cross section.

On the other hand, at a laser intensity of 5.1×10^4 W/cm^2, a melting mark was observed on the surface of the substrate. Additionally, there was a region where the crystal grains were refined on the cross section. This intensity corresponded to the threshold where the copper layer was formed on the substrate. Under the condition where the copper layer formed, the width of the melting mark corresponded to the width of the copper layer.

As a result of the bead-on test, the crystal grains were refined in the molten layer. In the conventional laser cladding method, there is a region where crystal grains changed [22]. However, an area where crystal grains changed was not observed in Fig. 3c, d, or e. Hence, copper layer formation was realized with a minimum molten layer on the substrate.

Figure 5 shows the cross-sectional area and powder mass efficiency as functions of laser intensity. The cross-sectional area and the powder mass efficiency increased as the laser intensity increased. The powder mass efficiency had the greatest value of 9.68% in the experiments.

4 Discussion

4.1 Heating of the powder in multi-beam laser cladding

To calculate the ratio of powder that is melted on the fly, the powder temperature should be considered. In this study, two laser modules are evaluated for simplicity. Figure 6 schematically diagrams multi-beam laser cladding. The substrate

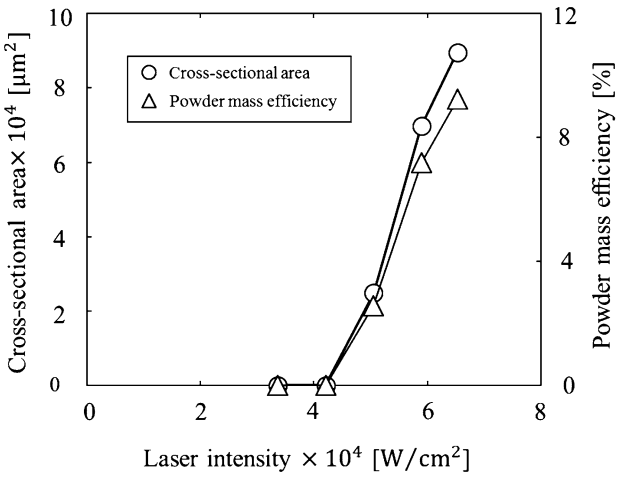

Fig. 5 Cross-sectional area S_{layer} and powder mass efficiency e_p of the copper layer as functions of laser intensity

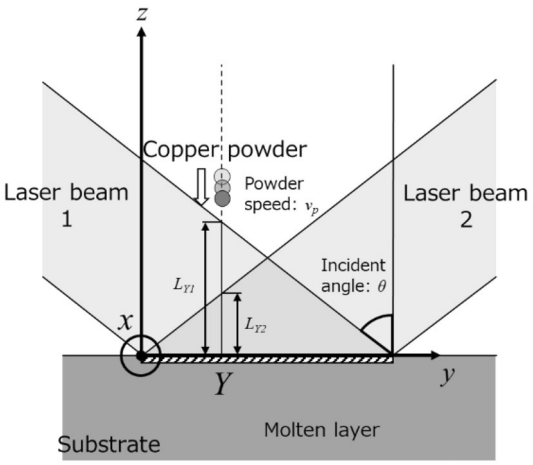

Fig. 6 Schematic of the multi-beam laser cladding method

is placed on the $x-y$ plane, and the blue laser beams are irradiated at an incident angle θ. Pure copper powder is supplied perpendicular to the substrate. All the copper powder passes through the rim and the top of the laser beams to the substrate. Therefore, the powder temperature is calculated under the following conditions:

- The laser intensity distribution is constant;
- The powder moves linearly at a constant speed;
- The powder temperature is uniform;
- Laser beams 1 and 2 have same intensity.
- The powder flow has a low optical density so as no shadowing or reduction in intensity occurs.

The copper powder receives energy by laser irradiation on the fly. The laser–powder interaction time t is given as follows using the interaction length L and the powder speed v_p

$$t = \frac{L}{v_\mathrm{p}} \tag{1}$$

The energy Q_p that the powder receives by laser irradiation on the fly is given by

$$Q_\mathrm{p} = A\frac{\pi d_\mathrm{p}^2}{4}It = \frac{\pi A d_\mathrm{p}^2 IL}{4v_\mathrm{p}} \tag{2}$$

where A is the laser absorptivity, d_p is the diameter of the copper powder, and I is the laser intensity of laser beam 1 or 2 shown in Fig. 6. The energy Q_p can also be expressed using the temperature rise ΔT as

$$Q_\mathrm{p} = mc\Delta T = \frac{\pi d_\mathrm{p}^3 \rho}{6} c\left(T_\mathrm{p} - T_0\right) \tag{3}$$

where m is the mass of powder, c is the specific heat, ρ is the density, T_p is the powder temperature when reaching the substrate, and T_0 is the initial temperature (room temperature). From Eqs. (2) and (3), the powder temperature T_p is given as

$$T_p = \left(\frac{3A}{2\rho_p c_p}\right)\left(\frac{I}{v_p d_p}\right)L + T_0 \tag{4}$$

In the case of a multi-beam laser cladding system, the powder is heated by laser beam 1 and 2 similar to Fig. 6. Let L_{Y1} and L_{Y2} represent the interaction length with the respective laser beams, and the total interaction length L is given as their sum

$$L = L_{Y1} + L_{Y2} = \frac{d_L - Y}{\tan\theta} + \frac{Y}{\tan\theta} = \frac{d_L}{\tan\theta} \tag{5}$$

Regardless of position Y, the total interaction length is constant. From Eqs. (4) and (5), the powder temperature T_p can be expressed as

$$T_p = \left(\frac{3A}{2\rho_p c_p}\right)\left(\frac{d_L I}{v_p d_p \tan\theta}\right) + T_0 \tag{6}$$

Equation (6) shows that all powder particles are heated uniformly by laser irradiation. Hence, a pure copper layer can be formed without dilution.

5 Temperature of copper powder

To consider the temperature of the powder, it is necessary to measure the powder speed in Eq. (1). Here, the powder speed is measured by a high-speed video camera (NAC, Memcam Q1v) and a metal halide lamp. The powder supplied from the nozzle is captured under the condition of 1.5×10^4 fps and the shutter speed of 5×10^{-5} s. The average speed of 30 particles is recorded as 7620 mm/s.

The powder temperature T_p is calculated by Eq. (6). Table 2 shows the calculation conditions. The light absorption rate of pure copper at a wavelength of 450 nm is 64% [22]. The laser spot diameter is based on the measurement results of the laser beam profile. Figure 7 plots the powder temperature as a function of laser intensity. The pure copper powder with a diameter of 15 μm or less is melted by laser irradiation at a laser intensity of 6.5×10^4 W/cm^2 based on the model, which corresponds to about 5% in the supplied powder. At the laser intensity of 5.9×10^4 W/cm^2, the pure copper powder with a diameter of 13 μm or less is melted, which is less than 5%. At the laser intensity of 5.1×10^4 W/cm^2, the pure copper powder with a diameter of 10 μm or less is melted. However, there is no powder under 10 μm in the supplied powder.

Table 2 Calculation conditions

Laser absorptivity A_p [-]	0.64
Density ρ_p [g /cm^3]	8.94
Specific heat c_p [J/(g·K)]	0.379
Laser spot diameter d_L [μm]	534
Powder speed v_p [mm/s]	7620
Melting temperature T_m [°C]	1084
Incident angle θ [°]	23
Initial temperature T_1 [°C]	21

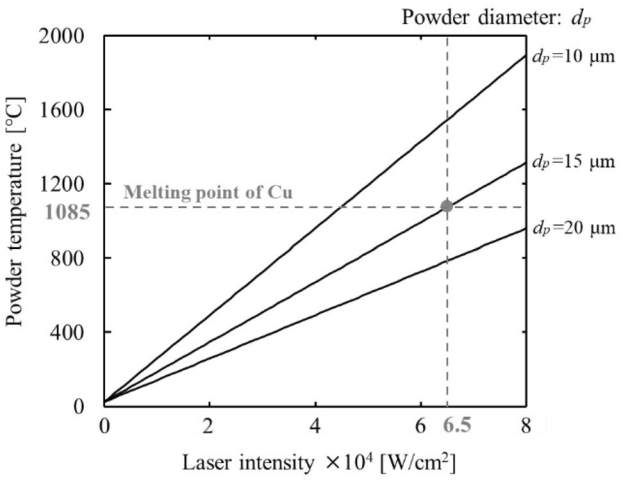

Fig. 7 Powder temperature as a function of laser intensity

Some powder reaches the substrate in the solid state. This unmelted powder is captured on the molten layer shown in Fig. 4b and is subsequently melted by laser irradiation or heat conduction. At a laser intensity of 4.2×10^4 W/cm^2 or less, the molten layer is formed on the substrate, and the layer does not bond to the substrate. At a laser intensity of 5.1×10^4 W/cm^2 or above, the molten layer forms on the substrate. Since only the powder supplied into the molten layer is bonded to the substrate, the copper layer width corresponds to the width of the molten region formed by laser irradiation without a powder supply.

6 Summary

A pure copper layer is formed on a pure copper substrate with a high-intensity blue diode laser installed in a multi-beam laser cladding system. The powder mass efficiency increases as the laser intensity increases. Based on these results, a powder temperature model is constructed. At a laser intensity of 6.5×10^4 W/cm^2, 9.65% of the powder forms a copper layer. In the supplied powder, approximately 5% of the powder is melted on the fly. In addition, about 5% of the powder melts after being trapped on the substrate. Hence, both the melted powder on the fly and the powder trapped on the substrate form the copper layer.

References

1. C. Yao, B. Xu, X. Zhang, J. Huang, J. Fu, Y. Wu, Interface microstructure and mechanical properties of laser welding copper-steel dissimilar joint. Opt. Lasers Eng. **47**, 807–814 (2009)
2. K. Mori, H. Murase, M. Kawasaki, T. Saito, Y. Shimura, New copper based composite for engine valveseat directly deposited onto aluminium alloy using laser cladding process. Laser cladding ho wo mochiita setsugo type valve seat yo doki fukugo zairyo no kaihatsu. Materia Japan **33**(4), 429–431 (1994)
3. M. Khalid Imran et al., Bimetallic dies with direct meta-deposited steel on Moldmax for high-pressure die casting application. Int. J. Adv. Manuf. **52**, 855–863 (2011)
4. F. Molledaa et al., Copper coating of carbon steel by a furnace brazing process using brass as the braze. Mater. Charact. **59**, 613–617 (2008)
5. O. Sharifahmadian et al., Relationship between surface properties and antibacterial behavior of wire arcspray copper coating. Surf. Coat. Technol. **233**, 74–79 (2013)
6. Xu Goujian et al., Comparison between diode laser and TIG cladding of Co-based alloys on the SUS403 stainless steel. Surf. Coat. Technol. **201**, 1138–1144 (2006)
7. A. Sova et al., Preliminary study on deposition of aluminum and copper powders by cold spray micronozzle using helium. Surf. Coat. Technol. **220**, 98–101 (2013)
8. I. Hemmati, V. Ocelik, J.T.M. De Hosson, Dilution effects in laser cladding of Ni–Cr–B–Si–C hardfacing alloys. Mater. Lett. **84**, 69–72 (2012)
9. Y. Wang, S. Zhao, W. Gao, C. Zhou, F. Liu, X. Lin, Microstructure and properties of laser cladding FeCrBSi composite powder coatings with higher Cr content. J. Mater. Process. Technol. **214**, 899–905 (2014)
10. A. Calleja, I. Tabernero, A. Fernández, A. Celaya, A. Lamikiz, L.L. de Lacalle, Improvement of strategies and parameters for multi-axis laser cladding operations. Opt. Lasers Eng. **56**, 113–120 (2014)
11. B. Song, T. Hussain, K.T. Voisey, Laser cladding of Ni50Cr: A parametric and dilution study. Phys. Proc. **83**, 706–715 (2016)
12. J. Yin, D. Wang, L. Meng, L. Ke, Q. Hu, X. Zeng, High-temperature slide wear of Ni–Cr–Si metal silicide based composite coatings on copper substrate by laser-induction hybrid cladding. Surf. Coat. Technol. **325**, 120–126 (2017)
13. K. Asano et al., Development of multiple laser beam irradiation method for precision laser cladding of metal. Rev. Laser Eng. **46**, 604–613 (2018)
14. K. Asano et al., Laser metal deposition of pure copper on stainless steel with blue and IR diode lasers. Opt. Laser Techonol. **107**, 291–296 (2018)
15. K. Asano et al., Copper film formation on metal surfaces with 100 W blue direct diode laser system. Laser appl. (2018). https://doi.org/10.2351/1.5040635
16. K.Toyoda et al., *Laser Handbook*, 2nd edn. (Ohmsha Ltd, 2005) p. 830 (**in Japanese**)
17. Ernie W. Spisz, Albert J. Weigand, Robert L. Bowman and John R. Jack, NASA Technical Note, NASA TN D-5353, pp. 1–21 (1969)
18. K. Morimoto, M. Tsukamoto, S. Masuno, K. Azumi, Y. Hayashi, N. Abe, Conference Proceedings of Lasers in Manufacturing (LiM) 2019, Munich, Germany (2019), p. 328
19. Y. Sato et al., In situ X-ray observations of pure-copper layer formation with blue direct diode lasers. Appl. Surf. Sci. **480**, 861–867 (2018)
20. K. Asano et al., Laser metal deposition of pure copper on stainless steel with blue and IR diode lasers. Opt. Laser Technol. **107**, 291–296 (2018)
21. M. Sengoku et. al. Experimental investigation on temperature distribution of molten pool for copper with blue direct diode laser cladding. in *Proceeding of ICALEO*, (2017), p 119
22. Shimadzu Corporation Expanded product line of short-wavelength lasers for materials processing and measuring applications—High-brightness blue direct diode laser also released to provide new techniques for microfabrication, (2014) https://www.shimadzu.com/about/pressrelease/5iqj1d0000020jc6.html. Accessed 12 Mar 2018